

Progress on Meson-Baryon Scattering

Colin Morningstar, a,* John Bulava, b Andrew D. Hanlon, c Ben Hörz, d Daniel Mohler, d Amy Nicholson, d Sarah Skinner d and André Walker-Loud d

E-mail: cmorning@andrew.cmu.edu

Progress in computing various meson-baryon scattering amplitudes is presented on a single ensemble from the Coordinated Lattice Simulations (CLS) consortium with $m_{\pi}=200$ MeV and $N_f=2+1$ dynamical fermions. The finite-volume Lüscher approach is employed to determine the lowest few partial waves from ground- and excited-state energies computed from correlation matrices rotated in a single pivot using a generalized eigenvector solution. This analysis requires evaluating matrices of correlation functions between single- and two-hadron interpolating operators which are projected onto definite spatial momenta and finite-volume irreducible representations. The stochastic LapH method is used to estimate all needed quark propagators. Preliminary results are presented for $I=\frac{1}{2},\frac{3}{2}$ $N\pi$ amplitudes including the $\Delta(1232)$ resonance and the I=0 S-wave amplitude with unit strangeness relevant for the $\Delta(1405)$.

The 38th International Symposium on Lattice Field Theory, LATTICE2021 26th-30th July, 2021 Zoom/Gather@Massachusetts Institute of Technology

^aDepartment of Physics, Carnegie Mellon University, Pittsburgh, PA, 15213, USA

^b Deutsches Elektronen-Synchrotron (DESY), Platanenallee 6, 15738, Zeuthen, Germany

^cPhysics Department, Brookhaven National Laboratory, Upton, New York, 11973, USA

^dNuclear Science Division, Lawrence Berkeley National Laboratory, Berkeley, CA, USA 94720

^eHelmholtzzentrum für Schwerionenforschung (GSI), Planckstrasse 1, 64291 Darmstadt, Germany

^f Department of Physics and Astronomy, University of North Carolina, Chapel Hill, NC, 27599, USA

^{*}Speaker

1. Overview

This talk is a progress report on our efforts to determine meson-baryon and baryon-baryon scattering parameters in a large number of flavor channels. Preliminary results from correlation matrices obtained using only one time source are presented for $I = \frac{1}{2}, \frac{3}{2} N\pi$ amplitudes including the $\Delta(1232)$ resonance and the I = 0 S-wave amplitude with unit strangeness relevant for the $\Delta(1405)$ using the D200 ensemble from the Coordinated Lattice Simulations (CLS) consortium with $m_{\pi} = 200$ MeV and $N_f = 2 + 1$ dynamical fermions. Results from correlators estimated using four time sources will soon be available.

Some motivations for this work are as follows. Meson-baryon amplitudes are useful for a variety of phenomenological applications both at the physical pion mass $m_\pi^{\rm phys}$ and for chiral effective field theories (EFT) at varying pion masses m_π . The process $\Delta(1232) \to N\pi$ is sometimes used as a degree-of-freedom in some EFT's. The scattering lengths $a_{N\pi}^{I=3/2}$ and $a_{N\pi}^{I=1/2}$ will impact the discrepancy between lattice QCD and phenomenology determinations for $\sigma_{\pi N}$, which is relevant for dark matter direct detection. Lattice QCD is a good laboratory to study the $\Lambda(1405)$ by varying quark masses.

2. Methodology

The finite-volume Lüscher approach[1–4] is employed to determine the lowest few partial waves from ground- and excited-state energies computed from correlation matrices rotated in a single pivot using a generalized eigenvector solution. Our implementation of the Lüscher method uses the "box matrix" *B* introduced in Ref. [5], along with the scattering *K*-matrix, to form the energy quantization condition. Parameters in the *K*-matrix are determined using the determinant residual method of Ref. [5]. This analysis requires evaluating matrices of correlation functions between single- and two-hadron interpolating operators which are projected onto definite spatial momenta and finite-volume irreducible representations. The stochastic LapH method[6] is used to estimate all needed quark propagators.

Finite-volume stationary-state energies are obtained from temporal correlations $C_{ij}(t) = \langle 0|\overline{O}_i(t)O_j(0)|0\rangle$, where $O_j(t)$ are appropriate single- and multi-hadron operators. In finite volume, such energies are discrete, so the correlators can be expressed in terms of the energies using

$$C_{ij}(t) = \sum_{n} Z_i^{(n)} Z_j^{(n)*} e^{-E_n t}, \qquad Z_j^{(n)} = \langle 0 | O_j | n \rangle, \tag{1}$$

ignoring negligible effects from the temporal boundary. It is not practical to do fits using the above form, so we define a new correlation matrix $\widetilde{C}(t)$ using a single-pivot rotation

$$\widetilde{C}(t) = U^{\dagger} C(\tau_0)^{-1/2} C(t) C(\tau_0)^{-1/2} U,$$
 (2)

where the columns of U are the eigenvectors of $C(\tau_0)^{-1/2} C(\tau_D) C(\tau_0)^{-1/2}$. We choose τ_0 and τ_D large enough so that $\widetilde{C}(t)$ remains diagonal for $t > \tau_D$ and such that the extracted energies are insensitive to increases in these parameters. Two-exponential fits to the diagonal elements $\widetilde{C}_{\alpha\alpha}(t)$ yield the energies E_{α} and overlaps $Z_j^{(n)}$. However, energy shifts from non-interacting levels can be more accurately obtained using single-exponential fits to suitable *ratios* of correlators.

It is extremely important to use judiciously constructed operators $O_j(t)$. Our operator construction is detailed in Refs.[7, 8]. Individual hadron operators are constructed using basic building blocks which are covariantly-displaced LapH-smeared quark fields. Stout link smearing[9] is used for the displacements, and Laplacian-Heaviside (LapH) smearing is used for the quark fields:

$$\widetilde{\psi}_{a\alpha}(x) = S_{ab}(x, y) \, \psi_{b\alpha}(y), \qquad S = \Theta\left(\sigma_s^2 + \widetilde{\Delta}\right),$$
 (3)

where the three-dimensional gauge-covariant Laplacian $\widetilde{\Delta}$ is given in terms of the smeared link variables \widetilde{U} , and σ_s is a smearing cutoff which determines the number $N_{\rm ev}$ of LapH eigenvectors to retain. The quarks are combined into so-called elemental meson and baryon operators:

$$\overline{\Phi}_{\alpha\beta}^{AB}(\boldsymbol{p},t) = \sum_{\boldsymbol{x}} e^{i\boldsymbol{p}\cdot(\boldsymbol{x}+\frac{1}{2}(\boldsymbol{d}_{\alpha}+\boldsymbol{d}_{\beta}))} \delta_{ab} \, \overline{q}_{b\beta}^{B}(\boldsymbol{x},t) \, q_{a\alpha}^{A}(\boldsymbol{x},t), \tag{4}$$

$$\overline{\Phi}_{\alpha\beta\gamma}^{ABC}(\boldsymbol{p},t) = \sum_{\boldsymbol{x}} e^{i\boldsymbol{p}\cdot\boldsymbol{x}} \varepsilon_{abc} \, \overline{q}_{c\gamma}^{C}(\boldsymbol{x},t) \, \overline{q}_{b\beta}^{B}(\boldsymbol{x},t) \, \overline{q}_{a\alpha}^{A}(\boldsymbol{x},t), \tag{5}$$

then the hadron operators are superpositions of the elemental operators obtained by group-theory projections onto the irreducible representations (irreps) of the appropriate lattice symmetry group:

$$\overline{M}_{l}(t) = c_{\alpha\beta}^{(l)*} \overline{\Phi}_{\alpha\beta}^{AB}(t) \qquad \overline{B}_{l}(t) = c_{\alpha\beta\gamma}^{(l)*} \overline{\Phi}_{\alpha\beta\gamma}^{ABC}(t). \tag{6}$$

For an operator creating a definite momentum p, our operators transform according to irreps of the little group of p on a cubic lattice. For multi-hadron operators, it is very important to use superpositions of products of single-hadron operators of definite momenta. Spatially localized multi-hadron operators produce signals with large amounts of excited-state contamination. Our hadron operator construction is very efficient and generalizes to three or more hadrons. Note that to speed up our computations to achieve the statistics needed for extracting the low-lying energies required for our baryon-baryon scattering studies, we have not included any single hadron operators with quarks that are displaced from one another.

Including multi-hadron operators in our correlation matrices requires the use of time-slice to time-slice quark propagators. To make the calculations feasible, we resort to employing stochastic estimates of such quark propagators. The stochastic LapH method[6] is used. We introduce N_R vectors of Z_4 noise $\eta^{(r)}$ in the LapH subspace

$$\eta_{\alpha k}^{(r)}(t), \qquad t = \text{time}, \ \alpha = \text{spin}, \ k = \text{eigenvector number}.$$
 (7)

We carry out variance reduction using noise dilution, which introduces projectors $P^{(a)}$. Defining

$$\eta^{[a]} = P^{(a)}\eta, \qquad X^{[a]} = D^{-1}\eta^{[a]},$$
(8)

we obtain Monte Carlo estimates of the quark propagators via

$$D_{ij}^{-1} \approx \frac{1}{N_R} \sum_{r=1}^{N_R} \sum_{a} X_i^{(r)[a]} \eta_j^{(r)[a]*}.$$
 (9)

We define four dilution schemes:

$$P_{ij}^{(a)} = \delta_{ij}, \qquad a = 0, \qquad \text{(none)},$$

$$P_{ij}^{(a)} = \delta_{ij}\delta_{ai}, \qquad a = 0, 1, \dots, N-1, \text{ (full)},$$

$$P_{ij}^{(a)} = \delta_{ij}\delta_{a,Ki/N}, \qquad a = 0, 1, \dots, K-1, \text{ (interlace-}K),}$$

$$P_{ij}^{(a)} = \delta_{ij}\delta_{a,i \text{ mod }k}, \qquad a = 0, 1, \dots, K-1, \text{ (block-}K).}$$
(10)

Table 1: The various isospin channels we plan to study using the CLS D200 ensemble, and the number of correlators we will compute in each channel.

Isospin channel	D200 Number of Correlators	
I = 0, S = 0, NN	8357	
$I = 0$, $S = -1$, Λ , $N\overline{K}$, $\Sigma \pi$ (45 SH)	8143	
$I = \frac{1}{2}, \ S = 0, N\pi$	696	
$I = \frac{1}{2}, S = -1, N\Lambda, N\Sigma$	17816	
I = 1, S = 0, NN (66 SH)	7945	
$I=\frac{3}{2},\ S=0,\ \Delta,N\pi$	3218	
$I=\frac{3}{2},\ S=-1,\ N\Sigma$	23748	
$I = 0$, $S = -2$, $\Lambda\Lambda$, $N\Xi$, $\Sigma\Sigma$ (66 SH)	16086	
$I = 2, S = -2, \Sigma\Sigma$ (66 SH)	4589	
Single hadrons (SH)	33	

We apply dilutions to the time indices (full for fixed sources, interlace for relative sources), the spin indices (full), and the LapH eigenvector indices (interlace-16).

Our current computations make use of 2000 configurations of the CLS D200 ensemble, which employs a $64^3 \times 128$ lattice with spacing $a \sim 0.065$ fm and open boundary conditions in time. The quark masses are tuned such that $m_{\pi} \sim 200$ MeV and $m_{K} \sim 480$ MeV. For the LapH smearing, we use $N_{\rm ev} = 448$. We are currently extending our computations to include the following source times: $t_0 = 35$ forward, $t_0 = 64$ forward and backward, and $t_0 = 92$ backward. Our Wick contractions are efficiently performed using tensor contraction software which exploits common subexpression elimination[10, 11] and makes heavy use of threaded batched BLAS routines. The various isospin channels that we are computing are listed in Table 1, as well as the total numbers of correlators that we are computing in each channel.

Scattering parameters are extracted from finite-volume energies using our implementation[5] of the Lüscher method. We parametrize the inverse of the K-matrix, then determine best-fit values of the parameters using the determinant residual method[5] in which we minimize

$$\Omega(\mu, A) \equiv \frac{\det(A)}{\det[(\mu^2 + AA^{\dagger})^{1/2}]},\tag{11}$$

with $A = 1 - \widetilde{K}^{-1}B^{-1}$, where \widetilde{K} is the K-matrix with threshold factors removed, and B is the so-called box matrix. We typically use $\mu = 1$.

In this talk, we present preliminary results for $N\pi$ scattering in the isoquartet and isodoublet nonstrange channels using only one time source. Recall that the K-matrix has the form $K_{L'S'a';LSa}^{(J)}$. For one channel, a=a'=0, and for $N\pi$, we have total spin $S=S'=\frac{1}{2}$. Invariance under parity requires $(-1)^{L+L'}=1$ for $N\pi$, which is tantamount to L=L'. Hence, we can use the simplified notation $K_{L}^{(J)}$. Restricting to $L\leq 2$, the (2J,L) partial wave content of various blocks of the matrix $1-\widetilde{K}^{-1}B^{-1}$ are listed in Table 2. The elements of the scattering K-matrix which must be parametrized for $L\leq 2$ are also listed in Table 2.

Table 2: (Left) The (2J, L) partial wave content of various blocks of the matrix $1 - \widetilde{K}^{-1}B^{-1}$ labelled by little group irrep $\Lambda(d^2)$ for $N\pi$ states of $I = \frac{1}{2}, \frac{3}{2}$. Note that the integer d^2 refers to total momentum $P^2 = (2\pi/L_{\text{lat}})^2 d^2$ for a lattice volume L_{lat}^3 . (Right) The elements of the scattering K-matrix, denoted by $K_I^{(J)}$, which must be parametrized for $L \le 2$. See Ref. [8] for a description of the irrep labels.

$\Lambda(d^2)$	$(2J, L)$ content for $L \le 2$		
$H_g(0)$	(3, 1)		
$H_u(0)$	(3,2), (5,2)		
$G_{1g}(0)$	(1,1)		$J K_L^{(J)} \text{ needed for } L \le 2$
$G_{1u}(0)$	(1,0)	<i>J</i>	
$G_{2g}(0)$		1	$_{\mathbf{L}}(1/2)$ $_{\mathbf{L}}(1/2)$
$G_{2u}(0)$	(5,2)	$\frac{1}{2}$	$K_0^{(1/2)}, K_1^{(1/2)}$
$G_1(1), G_1(4)$	(1,0), (1,1), (3,1), (3,2), (5,2)	$\frac{3}{2}$	$K_1^{(3/2)}, K_2^{(3/2)}$
$G_2(1), G_2(4)$	(3, 1), (3, 2), (5, 2)	<u>5</u>	$K_2^{(5/2)}$
G(2)	(1,0), (1,1), (3,1), (3,2), (5,2)	<u> </u>	
$F_1(3)$	(3, 1), (3, 2), (5, 2)		
$F_2(3)$	(3, 1), (3, 2), (5, 2)		
G(3)	(1,0), (1,1), (3,1), (3,2), (5,2)		

The finite-volume energies are determined from ratio fits to single-pivot rotated correlators. Determinations of energy shifts Δ_E from non-interacting energies were checked for stability against variations of the single-pivot times (τ_0, τ_D) and on increasing the number of operators $n_{\rm ops}$. We parametrized resonant amplitudes with a Breit-Wigner form and used leading-order effective range expansions for non-resonant amplitudes, that is, parametrizing them with a constant. Covariance matrices and all statistical errors were estimated using bootstrap resampling with $N_B = 800$ samples. All elastic levels are included. Any level within 1σ of an inelastic threshold was not included. Parametrizations were provided for all S- and P-waves. Higher partial waves are ignored for now, but will be included in our final analyses. For the $\Lambda(1405)$ channel, we consider coupled channels with $\Sigma \pi$, $N\overline{K}$. Mixing of two-hadrons with stable hadrons is included in the $I=\frac{1}{2}$ and I=0, S=1 channels. The relevant stable hadron for $I=\frac{1}{2}$ is the nucleon, and for I=0, S=1, it is the $\Lambda(1115)$.

The finite-volume spectrum for $I=\frac{3}{2}$ is shown in Fig. 1, and the scattering phase shifts are shown in Fig. 2. Seventeen levels across $H_g(0)$, $G_{1u}(0)$, $G_{1}(1)$, G(2), $F_{1}(3)$, $F_{2}(3)$, $G_{1}(4)$, $G_{2}(4)$ are included in the analysis. The $G_{1g}(0)$ irrep which includes the leading (2J,L)=(1,1) wave is not included because the ground state in this irrep is inelastic. A Breit-Wigner form is used to parametrize $\widetilde{K}_1^{(3/2)}(E)$, and constants are used for $\widetilde{K}_0^{(1/2)}(E)$ and $\widetilde{K}_1^{(1/2)}(E)$. The best-fit results are

$$\frac{m_{\Delta}}{m_{\pi}} = 6.380(20), \quad g_{\Delta N\pi} = 13.7(1.5), \quad \chi^2/\text{d.o.f.} = 1.74,$$

$$m_{\pi} a_0^{J=1/2} = -0.254(41), \quad (m_{\pi} a_1^{J=1/2})^{-1} = 2.61(44).$$

The resonance parameters are consistent with a fit to *P*-wave only irreps.

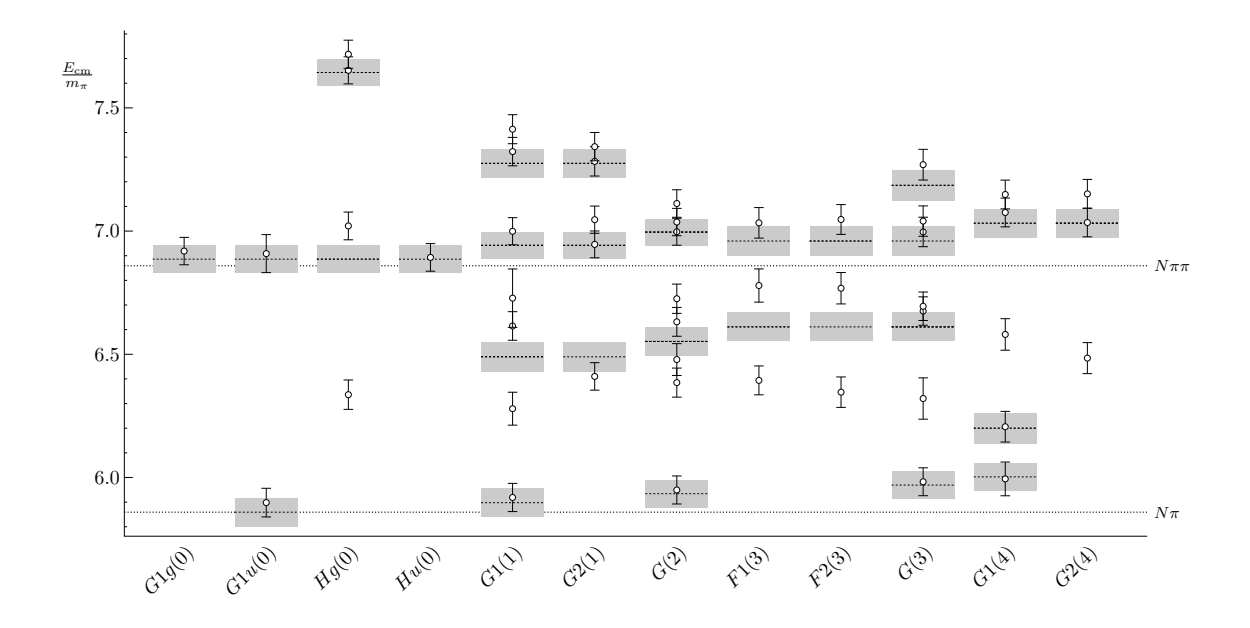


Figure 1: Center-of-mass energies $E_{\rm cm}$ as ratios over the pion mass m_{π} in the isoquartet non-strange sector for various little group irreps. The dashed horizontal lines show the non-interacting energies of the expected free two-particle states; the errors in the non-interacting energies are indicated by the gray boxes. The integers in parentheses in the irreps indicate d^2 for total momentum squared $P^2 = (2\pi/L)^2 d^2$.

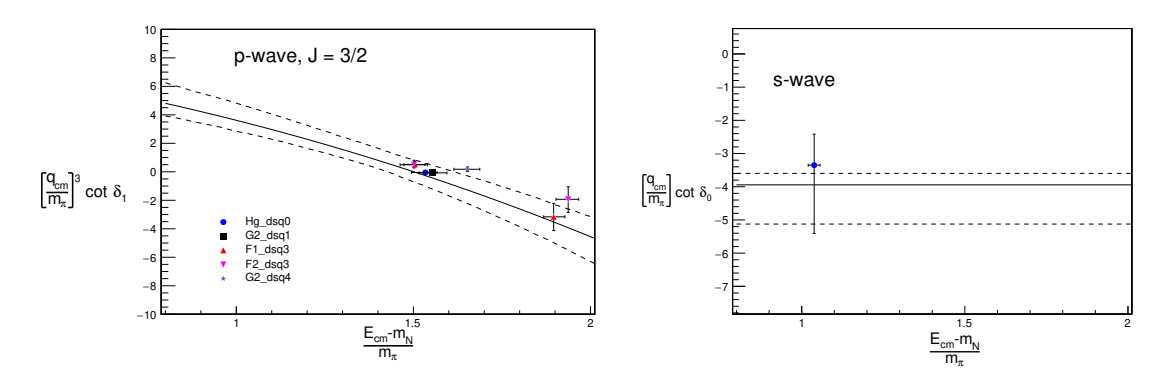


Figure 2: Threshold factors times cotangents of the phase shifts for the *P*-wave (left) and *S*-wave (right) for the isoquartet nonstrange channel against center-of-mass energies $E_{\rm cm}$ minus the nucleon mass M_N as a ratio over the pion mass m_π . Best-fit functions are shown as solid lines with error bands shown as dashed lines.

Two examples of extracting energy shifts in the isodoublet nonstrange channel are illustrated in the t_{\min} plots shown in Fig. 3. Each point is a fit using a single-exponential form to the single-pivot rotated correlator divided by the non-interacting level for time range from the t_{\min} shown on the horizontal axes to $t_{\max} = 25a$. Compared with the corresponding levels in the $I = \frac{3}{2}$ channel, the energy shifts are considerably smaller, as expected from the phenomenologically smaller value of the scattering length. A preliminary estimate of the $I = \frac{1}{2}$ scattering length $a_0^{1/2}$ is obtained by

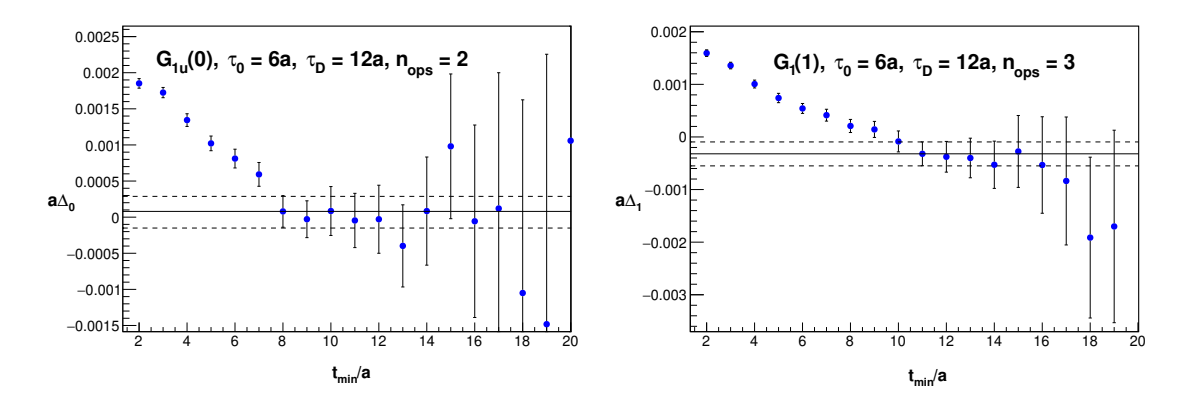


Figure 3: t_{min} plots for the energy shifts from non-interacting two-particle energies in terms of the lattice spacing a for the isodoublet nonstrange channel for the ground state in $G_{1u}(0)$ (left) and the first-excited state in $G_1(1)$ (right). The single-pivot rotation times τ_0, τ_D are indicated, and n_{ops} are the numbers of operators used in the correlation matrices. Fits using $t_{\text{min}} < 8$ have $\chi^2/\text{dof} > 2$.

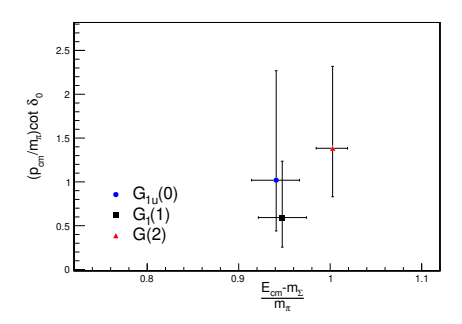


Figure 4: Preliminary estimates of the (2J, L) = (1, 0) S-wave scattering amplitude in the I = 0, S = 1(Lambda) channel. These results are obtained from the leading-partial wave approximate in the $G_{1\mu}(0)$, $G_1(1)$ and G(2) irreps using only the lowest scattering state, as discussed in the text.

ignoring $L \ge 1$ contributions in the quantization conditions for both levels,

$$(m_{\pi}a_0^{1/2})^{-1} = -86.06(72.14), \qquad G_{1u}(0), \tag{12}$$

$$(m_{\pi}a_0^{1/2})^{-1} = -86.06(72.14), \qquad G_{1u}(0),$$
 (12)
 $(m_{\pi}a_0^{1/2})^{-1} = 19.82(16.25), \qquad G_1(1).$ (13)

Additional statistics and a more complete analysis of the elastic spectrum for $I = \frac{1}{2}$ is required.

The final channel presented here is the I = 0, S = 1 channel, which is relevant for studying the $\Lambda(1405)$. This channel presents several additional difficulties. First, it may not be appropriate to truncate the quantization conditions at $L_{\text{max}} = 1$ due to the low-lying $\Lambda^*(1520)$ resonance in the (2J, L) = (3, 2) wave. Secondly, in order to accurately capture this excitation, it has been demonstrated [12] that three-quark operators with gauge-covariant derivatives are needed to capture the orbital structure. Such operators have not been included in our computations. Third, there are multiple coupled two-hadron scattering channels which are expected to mix significantly, the most important of which are $\Sigma \pi$ and $N\overline{K}$. These issues complicate the construction of correlation matrices, the extraction of levels, and the parametrization of the coupled-channel scattering amplitude in this flavor channel.

All of these difficulties are ignored in this progress report which presents only our preliminary estimates. Our results for the scattering amplitude using the S-wave approximation are shown in Fig. 4. Here, we assume that the lowest-lying $\Sigma\pi$ state is insensitive to the (2J,L)=(3,2) wave in the $G_1(1)$ and G(2) irreps, which also contain the (1,0) and (1,1) waves. Only the lowest $\Sigma\pi$ scattering state is included in each of the $G_{1u}(0)$, $G_1(1)$, and G(2) irreps. As in the $I=\frac{1}{2}$ channel, the ground state in each irrep of non-zero total momenta is the lowest-lying stable Λ , which is far below the two-particle scattering threshold and so these levels are not included in the analysis. Despite the large statistical errors, there is some encouraging indication that the $\Sigma\pi$ phase shift is positive.

For all of the results shown in this talk, we will soon present improved estimates using the increased statistics from including three more time sources and employing more comprehensive studies of the entire two-hadron spectra below the three-hadron thresholds, including all allowed types of two-hadron states.

Acknowledgments

Calculations for the results presented here were performed on the HPC clusters "HIMster II" at the Helmholtz-Institut Mainz, "Mogon II" at JGU Mainz, and "Frontera" at the Texas Advanced Computing Center (TACC). The computations were performed using the chroma_laph and last_laph software suites. chroma_laph uses the USQCD chroma [13] library and the QDP++ library. The contractions were optimized with contraction_optimizer [11]. The computations were managed with METAQ [14, 15]. The correlation function analysis was performed with chimera and SigMonD. We are grateful to our colleagues within the CLS initiative for sharing ensembles.

CJM acknowledges support from the U.S. NSF under award PHY-1913158. ADH is supported by the U.S. Department of Energy, Office of Science, Office of Nuclear Physics through the Contract No. DE-SC0012704 and within the framework of Scientific Discovery through Advance Computing (SciDAC) award "Computing the Properties of Matter with Leadership Computing Resources". AWL acknowledges support from the U.S. DOE through award number DE-AC02-05CH11231, an LBNL LDRD grant, and an Early Career Award. DM acknowledges funding by the Heisenberg Programme of the Deutsche Forschungsgemeinschaft (DFG, German Research Foundation), project number 454605793.

References

- [1] M. Luscher, Two particle states on a torus and their relation to the scattering matrix, Nucl. *Phys.* **B354** (1991) 531.
- [2] K. Rummukainen and S.A. Gottlieb, *Resonance scattering phase shifts on a nonrest frame lattice*, *Nucl. Phys.* **B450** (1995) 397 [hep-lat/9503028].
- [3] C.H. Kim, C.T. Sachrajda and S.R. Sharpe, *Finite-volume effects for two-hadron states in moving frames*, *Nucl. Phys.* **B727** (2005) 218 [hep-lat/0507006].
- [4] R.A. Briceno, *Two-particle multichannel systems in a finite volume with arbitrary spin, Phys. Rev.* **D89** (2014) 074507 [1401.3312].

- [5] C. Morningstar, J. Bulava, B. Singha, R. Brett, J. Fallica, A. Hanlon et al., *Estimating the two-particle K-matrix for multiple partial waves and decay channels from finite-volume energies*, *Nucl. Phys. B* **924** (2017) 477 [1707.05817].
- [6] C. Morningstar, J. Bulava, J. Foley, K.J. Juge, D. Lenkner, M. Peardon et al., *Improved stochastic estimation of quark propagation with Laplacian Heaviside smearing in lattice QCD*, *Phys. Rev. D* **83** (2011) 114505 [1104.3870].
- [7] S. Basak, R.G. Edwards, G.T. Fleming, U.M. Heller, C. Morningstar, D. Richards et al., Group-theoretical construction of extended baryon operators in lattice QCD, Phys. Rev. D 72 (2005) 094506.
- [8] C. Morningstar, J. Bulava, B. Fahy, J. Foley, Y.C. Jhang, K.J. Juge et al., *Extended hadron and two-hadron operators of definite momentum for spectrum calculations in lattice QCD*, *Phys. Rev. D* **88** (2013) 014511.
- [9] C. Morningstar and M. Peardon, *Analytic smearing of* SU(3) *link variables in lattice QCD*, *Phys. Rev. D* **69** (2004) 054501.
- [10] B. Hörz and A. Hanlon, *Two- and three-pion finite-volume spectra at maximal isospin from lattice QCD*, *Phys. Rev. Lett.* **123** (2019) 142002 [1905.04277].
- [11] B. Hörz, "Contraction optimizer." https://github.com/laphnn/contraction_optimizer, 2019.
- [12] S. Meinel and G. Rendon, $\Lambda_c \to \Lambda^*(1520)$ form factors from lattice QCD and improved analysis of the $\Lambda_b \to \Lambda^*(1520)$ and $\Lambda_b \to \Lambda_c^*(2595, 2625)$ form factors, 2107.13140.
- [13] SciDAC, LHPC, UKQCD collaboration, *The Chroma software system for lattice QCD*, *Nucl. Phys. B Proc. Suppl.* **140** (2005) 832 [hep-lat/0409003].
- [14] E. Berkowitz, "Metaq: Bundle supercomputing tasks." https://github.com/evanberkowitz/metaq, 2018.
- [15] E. Berkowitz, G.R. Jansen, K. McElvain and A. Walker-Loud, *Job Management and Task Bundling*, *EPJ Web Conf.* **175** (2018) 09007 [1710.01986].